

# **Development of Posture Prediction and Accommodation Models for Military Vehicles: Commander and Gunner Positions**

Matthew P. Reed  
Sheila M. Ebert

University of Michigan Transportation Research Institute

Final Report

UMTRI-2021-7

***September 2021***

**Technical Report Documentation Page**

1. Report No. UMTRI-2021-7	2. Government Accession No.	3. Recipient's Catalog No.	
4. Title Development of Posture Prediction and Accommodation Models for Military Vehicles: Commander and Gunner Positions		5. Report Date	
		6. Performing Organization Code	
7. Author(s) Reed, M.P. and Ebert, S.M.		8. Performing Organization Report No. UMTRI-2021-7	
9. Performing Organization Name and Address University of Michigan Transportation Research Institute 2901 Baxter Rd. Ann Arbor MI 48109		10. Work Unit No. (TRAIS)	
		11. Contract or Grant No.	
12. Sponsoring Agency Name and Address US Army Tank-Automotive Research and Development Center		13. Type of Report and Period Covered	
		14. Sponsoring Agency Code	
15. Supplementary Notes			
16. Abstract  Accurate information on warfighter posture and position is essential for the design of military vehicles for safety and effectiveness. In prior work, posture measurements from Soldiers were used to develop statistical posture-prediction and accommodation models for drivers in a range of configurations, including fixed heel point and fixed eye point. Models were also generated for a squad seating condition with no tasks. In the current study in the series, soldiers were measured in mockups representing commander and gunner positions. The commander position has an adjustable seatback angle, a keyboard, and a screen. The gunner condition is intended to simulate use of a remote weapons system and includes a seat with a fixed seat back angle, a joystick, and a screen. In each configuration, soldiers adjusted the screen and keyboard or joystick to obtain comfortable working postures, which were measured by recording the three-dimensional locations of body landmarks. Data were gathered with two ensembles: body armor vest and helmet (PPE level) and with the addition of a simulated body borne gear (BBG) rifleman kit representing the encumbered (ENC) soldier. Internal joint center locations were estimated from surface landmarks. Statistical posture-prediction models were developed using regression analysis to predict the locations of important landmarks, such as the hip joint centers, eyes, and knees. Population accommodation models were developed using parametric techniques developed in prior work. These models generate surface contours that can be used in design to accommodate a desired percentage of a vehicle occupant population. The models take into account the effects of population anthropometry, clothing and gear ensemble, and vehicle configuration. Contours were generated for the preferred and acceptable ranges of screen, keyboard, and joystick locations as well as eye location (eyellipse) and clearance contours for helmet, torso, elbow, knee, and boot.			
17. Key Word anthropometry, vehicle seats, posture, seat index point, H-point, human accommodation reference point		18. Distribution Statement	
19. Security Classif. (of this report)	20. Security Classif. (of this page)	21. No. of Pages 64	22. Price

## Metric Conversion Chart

### APPROXIMATE CONVERSIONS TO SI UNITS

SYMBOL	WHEN YOU KNOW		MULTIPLY BY	TO FIND		SYMBOL
<b>LENGTH</b>						
<b>In</b>	inches		25.4	millimeters		mm
<b>Ft</b>	feet		0.305	meters		m
<b>Yd</b>	yards		0.914	meters		m
<b>Mi</b>	miles		1.61	kilometers		km
<b>AREA</b>						
<b>in<sup>2</sup></b>	square inches	645.2	square millimeters		mm <sup>2</sup>	
<b>ft<sup>2</sup></b>	square feet	0.093	square meters		m <sup>2</sup>	
<b>yd<sup>2</sup></b>	square yard	0.836	square meters		m <sup>2</sup>	
<b>Ac</b>	acres	0.405	hectares		ha	
<b>mi<sup>2</sup></b>	square miles	2.59	square kilometers		km <sup>2</sup>	
<b>VOLUME</b>						
<b>fl oz</b>	fluid ounces	29.57	milliliters		mL	
<b>gal</b>	gallons	3.785	liters		L	
<b>ft<sup>3</sup></b>	cubic feet	0.028	cubic meters		m <sup>3</sup>	
<b>yd<sup>3</sup></b>	cubic yards	0.765	cubic meters		m <sup>3</sup>	
NOTE: volumes greater than 1000 L shall be shown in m <sup>3</sup>						
<b>MASS</b>						
<b>oz</b>	ounces	28.35	grams		g	
<b>lb</b>	pounds	0.454	kilograms		kg	
<b>T</b>	short tons (2000 lb)	0.907	megagrams (or "metric ton")		Mg (or "t")	
<b>TEMPERATURE (exact degrees)</b>						
<b>°F</b>	Fahrenheit	5 (F-32)/9 or (F-32)/1.8	Celsius		°C	
<b>FORCE and PRESSURE or STRESS</b>						
<b>lbf</b>	poundforce	4.45	newtons		N	

<b>lbf/in<sup>2</sup></b>	poundforce per square inch	6.89	kilopascals	kPa
<b>LENGTH</b>				
<b>mm</b>	millimeters	0.039	inches	in
<b>m</b>	meters	3.28	feet	ft
<b>m</b>	meters	1.09	yards	yd
<b>km</b>	kilometers	0.621	miles	mi
<b>AREA</b>				
<b>mm<sup>2</sup></b>	square millimeters	0.0016	square inches	in <sup>2</sup>
<b>m<sup>2</sup></b>	square meters	10.764	square feet	ft <sup>2</sup>
<b>m<sup>2</sup></b>	square meters	1.195	square yards	yd <sup>2</sup>
<b>ha</b>	hectares	2.47	acres	ac
<b>km<sup>2</sup></b>	square kilometers	0.386	square miles	mi <sup>2</sup>
<b>VOLUME</b>				
<b>mL</b>	milliliters	0.034	fluid ounces	fl oz
<b>L</b>	liters	0.264	gallons	gal
<b>m<sup>3</sup></b>	cubic meters	35.314	cubic feet	ft <sup>3</sup>
<b>m<sup>3</sup></b>	cubic meters	1.307	cubic yards	yd <sup>3</sup>
<b>MASS</b>				
<b>g</b>	grams	0.035	ounces	oz
<b>kg</b>	kilograms	2.202	pounds	lb
<b>Mg (or "t")</b>	megagrams (or "metric ton")	1.103	short tons (2000 lb)	T
<b>TEMPERATURE (exact degrees)</b>				
<b>°C</b>	Celsius	1.8C+32	Fahrenheit	°F
<b>FORCE and PRESSURE or STRESS</b>				
<b>N</b>	Newtons	0.225	poundforce	lbf
<b>kPa</b>	Kilopascals	0.145	poundforce per square inch	lbf/in <sup>2</sup>

\*SI is the symbol for the International System of Units. Appropriate rounding should be made to comply with Section 4 of ASTM E380.

(Revised March 2003)



## **ACKNOWLEDGMENTS**

This research was supported by the U.S. Army. We thank our colleagues Gale Zielinski and Frank Huston of the Ground Vehicle Systems Center, who collaborated on all aspects of the project. Our data collection would not have been possible without the generous assistance of Kevin West and the generous participation of Soldiers from Fort Riley.

## CONTENTS

ACKNOWLEDGMENTS .....	4
ABSTRACT.....	6
INTRODUCTION .....	7
METHODS .....	8
RESULTS: POSTURE PREDICTION MODELS .....	22
RESULTS: POPULATION ACCOMMODATION MODELS .....	30
DISCUSSION.....	43
REFERENCES .....	44
APPENDIX A. PARTICIPANT INTERACTION SCRIPTS .....	46
APPENDIX B. GENERAL CALCULATION METHODS FOR ACCOMMODATION MODELS .....	51
APPENDIX C. DRIVER ANTERIOR TORSO CONTOURS .....	54
APPENDIX D. HELMET CONTOURS .....	60

## ABSTRACT

Accurate information on warfighter posture and position is essential for the design of military vehicles for safety and effectiveness. In prior work, posture measurements from soldiers were used to develop statistical posture-prediction and accommodation models for drivers in a range of configurations, including fixed heel point and fixed eye point. Models were also generated for a squad seating condition with no task. In the current study in the series, soldiers were measured in mockups representing commander and gunner positions. The commander position has an adjustable seatback angle, a keyboard, and a screen. The gunner condition is intended to simulate use of a remote weapons system and includes a seat with a fixed seat back angle, a joystick, and a screen. In each configuration, soldiers adjusted the screen and keyboard or joystick to obtain comfortable working postures, which were measured by recording the three-dimensional locations of body landmarks. Data were gathered with two ensembles: body armor vest and helmet (PPE level) and with the addition of a simulated body borne gear (BBG) rifleman kit representing the encumbered (ENC) soldier. Internal joint center locations were estimated from surface landmarks. Statistical posture-prediction models were developed using regression analysis to predict the locations of important landmarks, such as the hip joint centers, eyes, and knees. Population accommodation models were developed using parametric techniques developed in prior work. These models generate surface contours that can be used in design to accommodate a desired percentage of a vehicle occupant population. The models take into account the effects of population anthropometry, clothing and gear ensemble, and vehicle configuration. Contours were generated for the preferred and acceptable ranges of screen, keyboard, and joystick locations as well as eye location (eyellipse) and clearance contours for helmet, torso, elbow, knee, and boot.

## INTRODUCTION

This report is one of a series documenting research to develop modern human-centered design tools for military vehicles (Zerehsaz et al. 2014a, 2014b; Reed and Ebert 2020). For each project, we have gathered posture, position, and adjustment data from Soldiers sitting in mockups of vehicle interior environments. The data are analyzed to develop statistical models predicting posture and accommodation requirements for individuals and populations as a function of Soldier and vehicle characteristics.

The current report focuses on non-driver workstations with two configurations. The commander position includes a seat with an adjustable back angle, a keyboard, and a screen. The gunner position, intended to represent a remote weapons operation station, included fixed seat back angle and adjustable joystick and screen components. In prior studies, we recorded Soldier's preferred locations for adjustable components. In the current study, we recorded both preferred and acceptable positions for the controls and displays were measured. The acceptable ranges are smaller than the preferred ranges to facilitate trade studies.

The data for the current study were gathered from 112 Soldiers at Fort Riley, Kansas in the spring of 2019. Trained investigators obtained standard anthropometric dimensions and measured body landmark locations as the Soldiers sat in a range of configurations in each mockup. The data were analyzed using statistical techniques developed in earlier work to produce posture-prediction and population accommodation models. The posture-prediction models give the most likely component adjustments, body landmark locations, and segment orientations as function of Soldier body dimensions and the vehicle layout. These models are used to posture human figure models that represent Soldiers of specific sizes. The population accommodation models are based on the same analysis but incorporate the population variance to produce statistical representations of the boundaries of Soldier preferences for component adjustment ranges as well as space claim for the head, torso, knees, elbows, and boots. Population accommodation models are used to assess current designs and as design guidance for future vehicles.

## **METHODS**

### **Human Research Approval**

The study protocol was approved by a University of Michigan Institutional Review Board (HUM00160030) and by the USAMRMC Office of Research Protections Human Research Protection Office (HRPO). Written informed consent was obtained from each participant.

### **Data Collection Site**

The Army provided access to facilities at Fort Riley, Kansas. The equipment, which was developed and fitted at UMTRI, was shipped to the base and set up by UMTRI staff. Data collection was conducted during Spring 2019. Soldiers were invited to participate by local personnel at each base. By design, the subject pool was not recruited to match a particular profile. Rather this convenience sample was intended to provide a broad range of human variability that is not necessarily representative of any particular part of the Army. The analysis methods enable the results to be tailored to any desired component of the current or future Army.

### **Standard Anthropometry**

Anthropometric data were gathered from each Soldier to characterize overall body size and shape following the procedures documented in Hotzman et al. (2011) for the ANSUR II survey. Standard anthropometric measures were obtained using manual measurements. The measurements included the core subset of dimensions gathered in ANSUR II. Table 1 lists the dimensions along with their corresponding identification in ANSUR II. All measurements were obtained with the Soldiers wearing their PT shorts, except that stature was measured with and without boots to characterize heel height. Tables 2 and 3 list summary statistics for selected anthropometric dimensions for Soldiers measured in each of the mockups.

Table 1  
Standard Anthropometric Measures

	Measurement	Posture	ANSUR II
1	Weight		6.4.92
2	Tragion to Top of Head	Sitting	6.4.83
3	Head Length	Sitting	6.4.48
4	Head Breadth	Sitting	6.4.46
5	Erect Sitting Height	Sitting	6.4.72
6	Eye Height	Sitting	6.4.35
7	Acromial Height	Sitting	6.4.2 (standing)
8	Knee Height	Sitting	6.4.58
9	Popliteal Height	Sitting	6.4.67
10	Acromial Breadth	Sitting	6.4.9
11	Bideltoid Breadth	Sitting	6.4.12
12	Maximum Hip Breadth	Sitting	6.4.52
13	Buttock-Knee Length	Sitting	6.4.20
14	Buttock-Popliteal Length	Sitting	6.4.21
15	Acromion – Radiale Length	<i>Sitting</i>	6.4.3 (standing)
16	Forearm – Hand Length	<i>Sitting</i>	6.4.41 (standing)
17	Stature Without Boots	Standing	6.4.76
18	Stature With Boots	Standing	
19	Chest Circumference (max anterior pt)	Standing	6.4.25
20	Waist Circumference at Omphalion	Standing	6.4.88
21	Hip Circumference at Buttocks	Standing	6.4.17
22	Bispinous Breadth	Standing	

Table 2  
Anthropometry Summary, Commander Position (81 men, 28 women)

Variable	Min	Mean	SD	Max
Stature	1470.0	1702.6	98.5	1956.0
Weight (kg)	17.9	26.3	3.7	38.1
BMI (kg/m <sup>2</sup> )	44.2	76.8	15.0	124.1
Age (yr)	18.0	24.5	5.0	44.0

Table 3  
Anthropometry Summary, Gunner Position (67 men, 38 women)

Variable	Min	Mean	SD	Max
Stature	1470.0	1704.2	98.5	1956.0
Weight (kg)	17.9	26.4	3.7	38.1
BMI (kg/m <sup>2</sup> )	44.2	77.1	14.9	124.1
Age (yr)	18.0	24.5	5.1	44.0

### Ensemble Levels and Fitting

Testing was conducted in two ensemble levels selected to be the same as those used in the earlier studies. Figure 1 shows the ensemble levels. At the PPE (personal protective equipment) level, Soldiers wore an Improved Outer Tactical Vest (IOTV) with Enhanced Small Arms Protective Insert (ESAPI) plates, Enhanced Side Ballistic Inserts (ESBI), and an Advanced Combat Helmet (ACH) over their ACU ensemble. Five sizes of IOTV were available at the study site. Figure 2 shows a soldier selecting an IOTV. The Soldiers were given their self-reported sizes of helmet and IOTV with front, back and side plates. The investigator helped the Soldier don the PPE and checked the fit. Figures 3 and 4 show the try-on process. The fit was considered acceptable if (1) the elastic waistband of the IOTV was snug with the Velcro closure fully overlapped and (2) the bottom of the IOTV was located below the navel and above the belt. The Soldiers wore the smallest size helmet in which the Soldier's head was in contact with the padding on the inside of the top of the helmet.

The second level of gear was referred to as body-born gear (BBG) or encumbered (ENC), which consisted of ACU, PPE, a hydration pack, and a Tactical Assault Panel (TAP). Note that BBG/ENC is nominally identical to the rifleman ENC condition used in the earlier studies. The TAP is an adaptable platform intended to replace the Fighting Load Carrier (FLC) vest to allow for quick release of equipment in emergency situations (Figures 5 and 6). The TAP is designed to carry a variety of basic Modular Lightweight Load-Carrying Equipment (MOLLE) fighting load pouches. The TAP was equipped with a harness that went over the head and around the sides. Unlike in the earlier studies, the hydration pack was not included.



Figure 1. The two ensemble levels, from left: PPE, and BBG (ENC) in the gunner position.

The rifleman's TAP represents the load of a rifleman, including a communications radio. Table 4 lists the items carried in the TAP. Targets were applied to the helmet and IOTV to facilitate tracking during testing (Figures 7 and 8). The locations of these targets were recorded in trials in which this gear was present.



Figure 2. Soldier in his ACU selecting IOTV





Figure 3. Testing IOTV fit and Soldier tightening ACH and checking size



Figure 4. Participant in BBG (ENC) ensemble.



Figure 5. TAP and hydration close up



Figure 6. TAP laid flat.

Table 4  
Inventory of Equipment in Rifleman BBG (ENC)

Item	Count
Replica M16 magazine clips	8
Replica Multiband Inter/Intra Team Radio (MBITR)	1
Replica fragmentation grenade	2
Multipliers	1
Canteen case with weight of night vision goggles added	1
Improved first aid kit (IFAK)	1
TAP with pouches	1

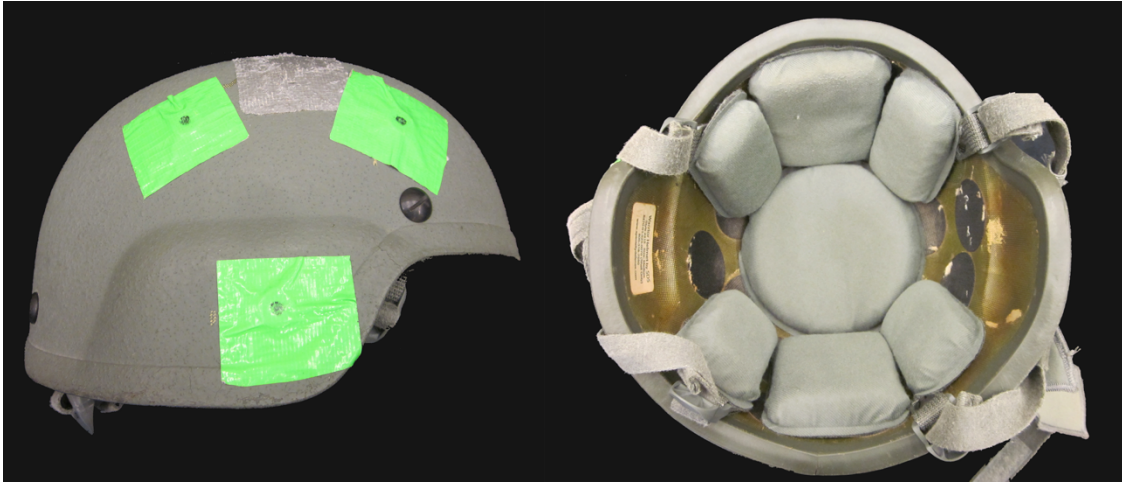


Figure 7. ACH with reference points and interior with pads configuration tested



Figure 8. IOTV with reference points

### **Participant Interaction Scripts**

Appendix A lists the participant interaction scripts for each mockup. These interaction scripts ensured that each participant received the same information and instructions.

### **Mockups and Test Conditions**

#### *Commander*

All data collection was conducted in the same mockup, with different components used depending on the condition. Figure 9 shows the mockup in the commander configuration.



The seat Human Accommodation Reference Point (HARP) was measured using the SAE J826 H-point machine (Figure 10). Note that the seat back angle in the mockup seat is taken to be equal to be the angle of the undeflected surface of the seat back with respect to vertical, which is equivalent to the H-point manikin torso angle when installed at midrange positions. The HARP was measured with the seat back angle at 17 degrees.

The seat height was set with the HARP 430 mm above the floor surface and the seat cushion angle at 5 degrees to horizontal. The screen center was fixed at 700 mm above HARP. The seat back angle was initially set to 10 degrees with respect to vertical but was adjusted by the participant to obtain a comfortable seated posture. After the participant was seated comfortably, the investigator adjusted the keyboard location to obtain the participant's preferred position. The keyboard was then moved forward and rearward (randomized order) to obtain the "maximum acceptable" deviations from preferred. The screen was then adjusted to the participant's preferred fore-aft position. During the screen adjustment process, the participant was required to reach with the left index finger to "button" targets at each corner of the screen, which displayed the static image shown in Figure 11. This ensured that the screen was reachable for touchscreen operations. The investigator then moved the screen fore-aft to obtain the maximum acceptable forward and maximum rearward positions, while maintaining the capability to reach to the corner buttons.

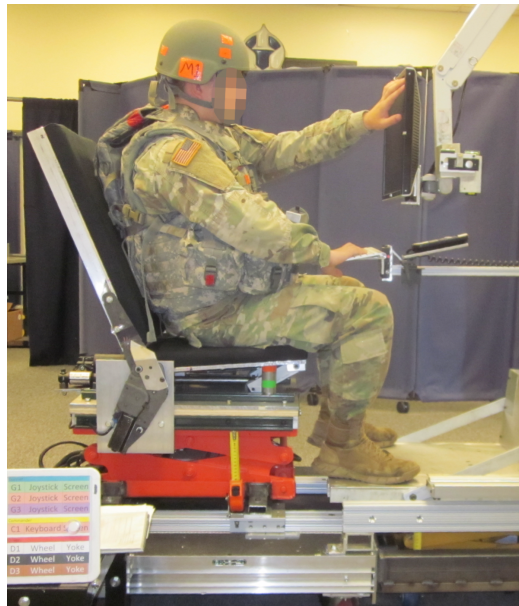


Figure 9. Commander configuration with keyboard and screen.



Figure 10. SAE J826 H-point machine in test seat (weights not shown).



Figure 11. Keyboard and static image displayed in the commander condition. The participant was required to touch the red (corner) buttons with their right index finger in all screen locations.

## Gunner

Figure 12 shows the mockup with the components used for the gunner conditions. The joystick was mounted to the right of the participant on a fixture that provided fore-aft, lateral, and vertical adjustability. The screen displayed the static image shown in Figure 13. Seat height was fixed with the HARP 450 mm above the floor surface. The seat back angle was set to 0, 10, or 20 degrees to vertical; these were associated with seat cushion angles of 0, 5, and 10 degrees above horizontal, respectively (i.e., seat cushion angle is one-half of seat back angle). All trials were conducted with the PPE ensemble, and the 10-degree seat back angle condition was repeated with the BBG (ENC) ensemble. The center of the screen was set 670 mm above HARP. The joystick center was set to 210 mm above HARP for all conditions.

In each condition, the participant first obtained a comfortable posture. The investigator then assisted the participant in finding their preferred horizontal location for the joystick.

The posture was measured in this position. The investigator then assisted the participant in finding the most-forward, most-rearward, and most-outboard acceptable joystick positions, returning to the preferred position between each condition.

With the joystick in the preferred position, the investigator assisted the participant in locating their preferred fore-aft position for the screen. The participant was required to touch all four corners of the screen (red buttons in Figure 13) with the index finger of their left hand while selecting the screen position. The investigator then assisted the participant in locating the most forward and most rearward acceptable screen positions, repeating the requirement to touch all four corners of the screen with the left index finger while the right hand was on the joystick.

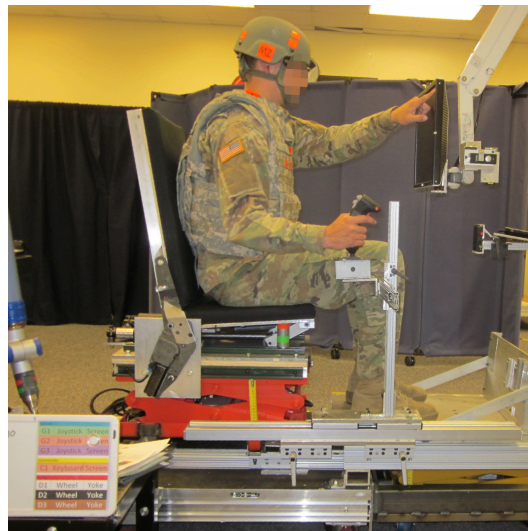


Figure 12 Gunner mockup.

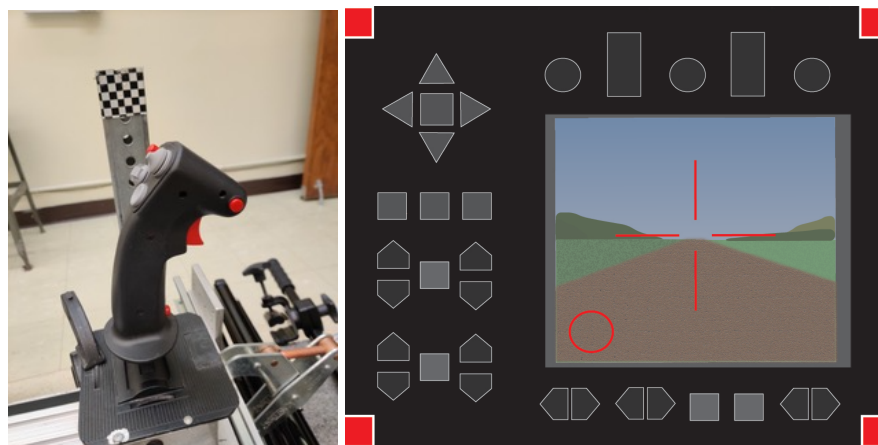


Figure 13. Joystick and static image presented on the screen in the gunner condition.

## Landmark Data

In each condition, the FARO Arm coordinate digitizer was used to record the three-dimensional location of the landmarks and reference points listed in Table 5. Figure 14 shows the FARO Arm being used to record landmark locations.

Table 5  
Landmarks and Reference Points Recorded in Mockups

C7 (Cervicale)	Most Forward Point on Torso
Back Of Head/Helmet Max Rearward	Most Lateral Point on Torso (Right)
Top Of Head/Helmet Max Height	Most Lateral Point on Thigh (Right)
Tragion (Right)	
Ectoorbitale (Right)	<b>On PPE and ENC</b>
Infraorbitale at Pupil Center (Right)	Helmet (3 Reference Points)
Glabella	IOTV (3 Reference Points)
Top of Hand Grip (Right)	TAP (3 Reference Points)
Ulnar Styloid Process (Right)	Camelbak (3 Reference Points)
Lateral Humeral Epicondyle (Right)	
Anterior-Superior Acromion (Right)	<b>On Equipment or Mockup</b>
Suprasternale (if reachable)	Faro Arm Cart (3 Reference Points)
Substernale (if reachable)	Mockup Platform (3 Reference Points)
ASIS (Right and Left)	Seat Cushion (2 Reference Points)
Estimate of Greater Trochanter (Right)	Seat Back (2 Reference Points)
Back of Pelvis Compressed (Right)	Foot Platform Height Point
Lateral Femoral Epicondyle (Right)	
Suprapatella (Right and Left)	<b>Condition Specific</b>
Infrapatella (Right)	Screen Center X, Z
Lateral Ball of Foot (Right)	Joystick reference points
Lateral Malleolus (Right)	Keyboard reference points
Heel (Bottom edge of sole at midline, Right)	
Toe (Bottom edge of sole, longest shoe point, Right)	

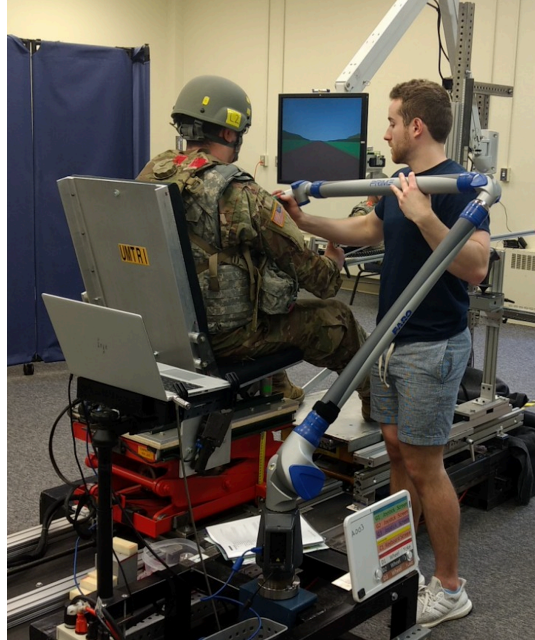


Figure 14. Using the FARO Arm to record posture.

### **Laboratory Hard Seat**

Data were also gathered from each participant in the laboratory hard seat shown in Figure 15. This seat allows posterior landmarks on the spine and pelvis to be measured along with the anterior landmarks that are accessible in the mockup seat. In the hard seat, participants wore athletic shorts and no shirt to facilitate landmark identification and measurement. The landmarks measured in the hard seat (Table 6) include a subset of those measured in the mockup in addition to a set of posterior spine and pelvis landmarks.





Figure 15. Hard seat

Table 6  
Landmarks and Reference Points Recorded in Hard Seat

Back Of Head (max rearward)	Acromion (Right and Left)
Top Of Head (Vertex)	Lateral Humeral Epicondyle (Left)
Tragion (Left)	Medial Humeral Epicondyle (Left)
Ectoorbitale (Left)	Ulnar Styloid Process (Left)
Infraorbitale at Pupil Center (Left)	Radial Styloid Process (Left)
Glabella	Suprasternale
Menton	Substernale
Lateral Femoral Epicondyle (Right and Left)	C7 (Cervicale)
Medial Femoral Epicondyle (Right and Left)	T4
Suprapatella (Right and Left)	T8
Infrapatella (Right and Left)	T12
Medial Malleolus (Left)	L1
Ball of Foot Medial (Left)	L2
Toe, Longest Tibiale (Left)	L3
Ball of Foot Lateral (Left)	L4
Lateral Malleolus (Left)	L5
Heel (Left)	
ASIS (Right and Left)	Hard Seat Platform (3 Reference Points)
PSIS (Right and Left)	Faro Arm Cart (3 Reference Points)

## Dependent Measures and Statistical Modeling

The calculation of dependent measures followed the methods in Reed and Ebert (2013). In brief, the hard seat data were used to estimate joint center locations in the spine, pelvis, and extremities to create a subject-specific kinematic linkage. This information was used with the landmarks obtained in the mockup conditions to estimate joint center locations.

Prior to statistical modeling, all of the data were expressed relative to the HARP location for the trial. All predicted values are with respect to HARP, except that knee landmark coordinates (*Z* axis values) are expressed with respect to the floor.

Statistical analyses were conducted using linear regression to estimate the location of important body landmarks and mockup components as a function of anthropometric and mockup variables. These methods followed those used in previous work (Reed and Ebert 2013). In particular, potential predictors were included if they were statistically significant with  $p < 0.01$  and their inclusion increased the adjusted  $R^2$  value for the regression by at least 0.02 (i.e., the variable accounted for at least two percent of the variance in the dependent measure).

Anthropometric predictors were stature, the ratio of erect sitting height to stature (SH/S), and body mass index (BMI,  $\text{kg}/\text{m}^2$ , computed as body weight in kg divided by stature in meters squared). The natural log ( $\ln$ ) of BMI was used rather than BMI because the

distribution of  $\ln(\text{BMI})$  is closer to a normal (Gaussian) distribution, which is valuable for population accommodation modeling.

## RESULTS: POSTURE PREDICTION MODELS

### Commander

Tables 7 through 10 list the regression models computed from the landmark and joint-center data. In each case, the complete regression equation is obtained by multiplying the coefficients by the predictors and summing together with the intercept. X is positive rearward of HARP, Y is positive to the occupant's right side, and Z is positive upward. The differential effects of PPE ensemble level compared with BBG (ENC) are listed as constant offsets (no interactions were significant). For example, the hips are 35 mm further rearward relative to HARP, on average, in the PPE condition than in the BBG (ENC) condition.

Table 11 shows the valid ranges of predictors based on the test conditions. Generally, seat heights above about 435 mm begin to cause disaccommodation for small women.

Table 7  
Regression Models for Posture Prediction: Commander

Variable (mm, deg)	Intercept	Stature	LnBMI (nat. log kg/m <sup>2</sup> )	SH/S	Garb** (PPE)	R <sup>2</sup> <sub>adj</sub>	RMSE
HipReHARPX	-295.7		66.2		35.5	0.30	30.3
HipReHARPZ	-82.7	0.0446			5.1	0.12	13.4
EyeReHARPX	78.0		-58.7		61.4	0.32	46.5
EyeReHARPZ	-44.8	0.2777	46.3	115.5		0.69	19.2
EyeReHipX	373.6		-124.9		25.9	0.14	52.2
EyeReHipZ	26.1	0.2350	45.2	134.4		0.49	24.8
HipEyeAngle	33.4		-11.2		2.3	0.14	4.6
HipEyeDistance	13.4	0.2393	47.6	134.3		0.51	24.7
SeatBackAngle*	-2.3	0.0124			-3.0	0.16	4.3
ThighSegmentAngle*	-41.0	0.0283			-3.0	0.47	2.9
LegSegmentAngle*†	0.8						9.4

\* Angles in degrees; Sitter-selected SeatBackAngle with respect to vertical as measured by Seat Index Point Tool or SAE J826 H-point manikin; ThighSegmentAngle is positive above forward horizontal.

\*\* Garb is PPE or BBG(ENC). Listed value is additive constant for PPE condition; use zero for BBG condition

† Leg segment angle is not significantly different from zero (vertical).

Table 8  
Regression Models for Body Segment Angles: Commander

Variable (deg)	Intercept	Hip-Eye Angle (deg aft of vertical)	Stature	R <sup>2</sup> <sub>adj</sub>	RMSE
PelvisSegmentAngle	-36.0	1.04	0.050	0.31	10.6
LumbarSegmentAngle	21.3	2.6		0.64	9.7
ThoraxSegmentAngle	-6.6	0.22		0.04	5.2
NeckSegmentAngle	13.5	0.61	-0.011	0.25	5.6
HeadNeckToTragionAngle	-2.6		-0.018	0.03	9.5
HeadSegmentAngle	34.5		-0.0179	0.05	7.7

Table 9  
Regression Models for Knee and Elbow Locations: Commander

Variable†	Intercept	Stature	LnBMI	GarbPPE	R <sup>2</sup> <sub>adj</sub>	RMSE
KneeX	-57.6	-0.2569		27.5	0.48	29.8
KneeY	-180.8	0.2247			0.24	39.5
KneeZ*	8.8	0.3045			0.73	18.3
ElbowX	98.4		-85.3	118.7	0.67	42.1
ElbowY	-167.8	0.1673	60.7	-31.9	0.55	22.7
ElbowZ	-72.5		102.3	-76.4	0.71	26.2

\* Wrt floor for seat height = 400 mm (should be independent of seat height over a reasonable range)

† Landmarks are suprapatellar (knee) and lateral humeral epicondyle (elbow).

Table 10  
Regression Models for Keyboard and Screen Locations: Commander

Variable	Intercept	Stature	LnBMI	GarbPPE	R <sup>2</sup> <sub>adj</sub>	RMSE
KeyPrefReHARPZ	18.9		57.5	-22.7	0.16	31.7
KeyForereHARPX	-92.1	-0.270		70.3	0.42	50.8
KeyPrefreHARPX	-226.7		-75.6	87.8	0.44	50.4
KeyAftreHARPX	-170.5		-78.0	110.0	0.60	45.5
ScreenForereHARPX	-122.5	-0.280		30.9	0.18	66.7
ScreenPrefreHARPX	-182.1	-0.210		30.1	0.17	56.3
ScreenAftreHARPX	-240.3	-0.138		34.7	0.11	60.3

\* Screen center height was fixed at 700 mm above H-point

Table 11  
Valid Range of Predictors for Commander Models

Predictor	Low Limit	High Limit	Acceptable Extrapolation	Cautions
Seat Height (HARP above Floor) (mm)	300	550	±50	Seat heights above about 435 mm will create disaccommodation for small drivers. This effect is not represented in the accommodation models
Stature (mm)	1450	2000	±10	
BMI (kg/m <sup>2</sup> )	20	32	±3	
SH/S (→)	0.50	0.54	0.01	

## Gunner

Tables 12 through 16 list the regression models for the gunner position. Note that data were gathered only in the PPE condition, so no ensemble effects are shown. Hip locations were slightly more rearward with greater seat back angle, and as expected eye locations were further rearward at higher seat back angles. Thigh segment angle was associated with stature, but the leg segment angle was not significantly different from vertical. Table 13 shows regression models for body segment angles as a function of body dimensions and the hip-eye vector angle. The resulting predictions are very similar to

those for other seating positions. Table 14 lists the regression models for knee and elbow locations. Seat back angle had small effects on the fore-aft locations of both the knees and elbows.

Table 12  
Regression Models for Posture Prediction: Gunner

Variable (mm, deg)	Intercept	Stature	LnBMI	SH/S	Seat Back Angle	R <sup>2</sup> <sub>adj</sub>	RMSE
HipReHARPX	96.4	-0.100			3.51	0.53	28.5
HipReHARPZ	-155.4	0.052	19.0		0.47		
EyeReHARPX	238	-0.226			6.93	0.77	32.3
EyeReHARPZ	-99.8	0.309	52.3	105.4		0.72	19.6
EyeReHipX	321.8	-0.112	-62.6		3.45	0.36	42.2
EyeReHipZ	62.5	0.256	31.9	106.4	-0.59	0.52	25.1
HipEyeAngle	26.8	-0.0092	-5.37		0.30	0.36	3.7
HipEyeDistance	50.7	0.261	34.8	104.1	-0.77	0.53	25.5
ThighSegmentAngle	-41.3	0.028				0.50	2.8
LegSegmentAngle*	--						

Table 13  
Regression Models for Body Segment Angles: Gunner

Variable (deg)	Intercept	Hip-Eye Angle	Stature	SH/S	R <sup>2</sup> <sub>adj</sub>	RMSE
PelvisSegmentAngle	-65.3	1.10	0.0531	43.3	0.27	10.6
LumbarSegmentAngle	20.3	2.66			0.65	8.9
ThoraxSegmentAngle	-6.1	0.228			0.04	5.1
NeckSegmentAngle	-4.1	0.600			0.18	5.8
HeadNeckToTragionAngle	-4.1		-0.017		0.04	8.3
HeadSegmentAngle	37.8		-0.020		0.16	4.4

Table 14  
Regression Models for Knee and Elbow Locations: Gunner

Variable	Intercept	Stature	LnBMI	SH/S	Seat Back Angle	R <sup>2</sup> <sub>adj</sub>	RMSE
KneeX	52.0	-0.320			3.19	0.69	27.0
KneeY	-257.2	0.190	35.7			0.29	30.6
KneeZ*	-3.4	0.314				0.78	16.3
ElbowX	-36.7				4.9	0.32	58.5
ElbowY	-217.9	0.081	116.8			0.41	22.5
ElbowZ	-360.7	0.046	118.7	134.8		0.31	27.2

\* Height above floor for seat height = 430 mm (should be independent of seat height over a reasonable range)

Table 15 lists the regression models for three different joystick positions: preferred, maximum acceptable forward, maximum acceptable aft (rearward), and maximum acceptable outboard (to the right of the gunner). The models refer to the estimated center of the joystick adjacent to the palm. Seat back angle generally affects both the fore-aft (X) and vertical (Z) locations and taller statures are associated with more-forward and more-outboard joystick locations.



Table 15  
Regression Models for Joystick Locations: Gunner

Variable	Intercept	Stature	LnBMI	Seat Back Angle	R <sup>2</sup> <sub>adj</sub>	RMSE
JoystickPrefReHARPX	248.6	-0.214	-79.2	4.77	0.35	62.0
JoystickPrefReHARPY	42.5	0.076	46.5		0.05	41.1
JoystickPrefReHARPZ	213.1			-0.30	0.29	3.8
JoystickForereHARPX	84.3	-0.355		5.94	0.57	52.3
JoystickForereHARPY	137.3	0.109			0.06	40.7
JoystickForereHARPZ	213.9			-0.29	0.30	3.6
JoystickAftreHARPX	36.6		-93.3	5.20	0.38	57.1
JoystickAftreHARPY	166.9	0.091		0.33	0.04	40.5
JoystickAftreHARPZ	212.2			-0.32	0.34	3.6
JoystickOutboardreHARPX	196.0	-0.212	-67.1	5.15	0.39	60.6
JoystickOutboardreHARPY	141.0	0.182			0.09	57.4
JoystickOutboardreHARPZ	211.1			-0.28	0.27	3.8

\*\* estimated palm-height center of joystick

Table 16 lists the regression models for fore-aft and vertical screen positions. The modeled landmark is the center of the screen. The models describe the preferred adjustment range as well as the smaller acceptable range. Increased seat back angle was associated with more-rearward and lower screen positions. Greater stature was associated with more-forward positions and higher positions. Note that Soldiers set the height of the screen only once, for the preferred condition at each seat back angle.

Table 16  
Regression Models for Screen Locations: Gunner

Variable	Intercept	Stature	Seat Back Angle	R <sup>2</sup> <sub>adj</sub>	RMSE
ScreenForeHARPX	-145.0	-0.291	6.14	0.43	66.2
ScreenForeHARPZ	655.8	0.010	-0.58	0.47	5.1
ScreenPrefHARPX	-192.3	-0.228	6.55	0.56	51.1
ScreenPrefHARPZ	674.2		-0.55	0.48	4.7
ScreenAftHARPX	-162.4	-0.199	5.96	0.50	52.7
ScreenAftHARPZ	673.0		-0.549	0.43	5.2

## RESULTS: POPULATION ACCOMMODATION MODELS

### Overview

The development of population accommodation models followed the general procedures presented in Reed and Ebert (2020) for driver workstations. The regression models presented above are used to predict mean responses for male and female sub-populations. The variance in the response (for example, eye location) is predicted by considering both anthropometric variation and the residual variation in the response that is not accounted for by the vehicle, seat, or anthropometric variables. This residual is represented by the root mean square error (RMSE) in the regression tables. (See Appendix B for general background on the mathematical formulation of accommodation models.)

Different accommodation models were developed for each seating position, depending on the constraints and variables in the test setup. Table 17 lists the models for each position.

Microsoft Excel workbooks have been created that embody these accommodation models. The Excel workbooks are considered to be the authoritative implementation of the accommodation models. If discrepancies are found between the Excel workbooks and this report, the Excel workbooks should take precedence. This report documents the procedures and differences among the models across seating configurations. For the examples, target accommodation was 90%.

Table 17  
Accommodation Model Availability by Seating Position

	Commander	Gunner
Eyellipse	X	X
Keyboard Position	X	
Screen Position	X	X
Joystick Position		X
Back Angle Adjustment	X	
Torso Contour	X	X
Helmet Contour	X	X
Knee Contour	X	X
Elbow Contour	X	X
Boot Contour	X	X

## Anthropometry Inputs

The anthropometry inputs are the same as in the previous model development work. Table 18 lists the inputs, which are the means and standard deviations of four variables for men and women. The values in Table 18 were obtained from ANSUR II, but values for any other population can be used as appropriate. In addition to these variables, the fraction of the population that is male is used in all calculations. In the examples in the sections that follow, the reference population is ANSUR II with 90% male.

Table 18  
Reference Anthropometric Inputs from ANSUR II

Dimension	Men		Women	
	Mean	SD	Mean	SD
Stature (S), mm	1756	68.6	1628	64.2
Erect Sitting Height (SH), mm	918	35.7	857	33.1
Erect Sitting Height / Stature (SHS)	0.523	0.0135	0.526	0.0141
Log(BMI)*, log(kg/m <sup>2</sup> )	3.31	0.146	3.23	0.135

\* Natural log; in Excel, use ln()

## Calibration and Ensemble Inputs

The clothing/gear ensemble is entered as PPE or ENC (BBG). Generally, ensemble affects fore-aft locations of all contours. The HARP can be established using either the SAE J826 H-point machine or the Seat Index Point Tool (SIPT). Choosing the SIPT shifts the estimated location of the HARP with respect to the seat by 5 mm; this effect is added into calculations related to fore-aft HARP location.

Table 19  
Inputs for Accommodation Models

Variable	Definition
Calibration Tool	SAE J826 H-point machine or Seat Index Point Tool. The SIP is assumed to lie 5 mm rearward of H-point. Either point is termed the Human Accommodation Reference Point (HARP) in the models.
Ensemble	ACU, PPE, or BBG (ENC)
Hydration Relief	Whether the seat has a cut-out for the hydration pack; if so, the ensemble level is considered to be PPE for purposes of hip location with respect to the seat

Seat Height	Used only for positioning the contours relative to the floor; not an input to posture prediction equations.
-------------	---

## Accommodation Models for Commander

### *Inputs*

For the examples below, a 90% male ANSUR II population was used. The ensemble level was set to PPE and the J826 manikin was used to establish HARP. The seat height was set to 450 mm and the seat was assumed to not have hydration pack relief.

### *Outputs*

Figure 16 shows the outputs of the commander accommodation models. The individual models are discussed below.

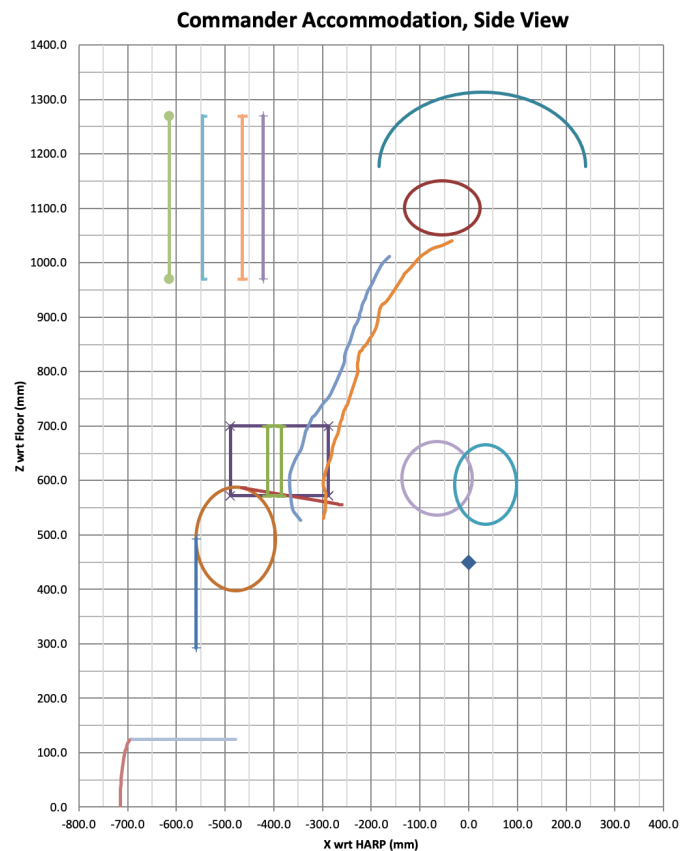


Figure 16. Side-view illustration of contours generated by commander accommodation models.

### *Eyellipse*

The commander eyellipse was derived using the same methods applied in the earlier squad accommodation study (Zerehsaz et al. 2015b). The eyellipse is aligned to grid, with the horizontal axis slightly longer than the vertical axis. Separate left and right eyellipses were generated using the standard 65-mm interpupillary distance from SAE J941. Figure 17 illustrates the eyellipses.

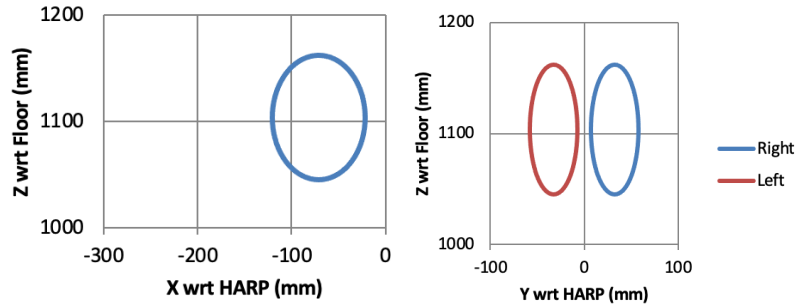


Figure 17. Commander eyellipse in sideview (left and rear view (right)).

*Seat Back Angle*

The distribution of sitter-selected seat back angle was modeled using the regression equation from Table 7. The residual variance was taken into account in the same manner as for the other univariate calculations. For 90% accommodation with the PPE ensemble level, the range is 14.5 degrees centered on 16.3 degrees, or 9.1 to 23.6 degrees.

*Torso Contour*

The torso contour represents a side-view and top-view contour for the PPE and ENC conditions. The contours, which were developed in prior work (Zerehsaz et al. 2014b), were positioned relative to HARP. To account for variability in torso posture, the contours were rotated around the HARP position by the difference between the predicted mean hip-eye angle (see Table 7) and the value obtained in the fixed-heel study (assumed constant at 1 degree aft of vertical). Table 20 lists the locating equations relative to HARP, adapted from the previous work. Figure 18 illustrate the torso contour outputs. The points defining the torso contours relative to the reference points are listed in Appendix C).

Table 20\*  
Locating Equations Relative to HARP for Torso Contour Reference Points: Commander

Reference Point	Constant	Stature	Ln(BMI)	SH/S	R <sup>2</sup> <sub>adj</sub>	RMSE
PPE-X	215		-92.9		0.23	25.1
PPE-Z	-408	0.156	119	349	0.71	13.3
ENC-X	-188.8	0.095	-75.2		0.13	31.7
ENC-Z	299					

\* Adapted from Table 7 in Zerehsaz et al. (2014b)

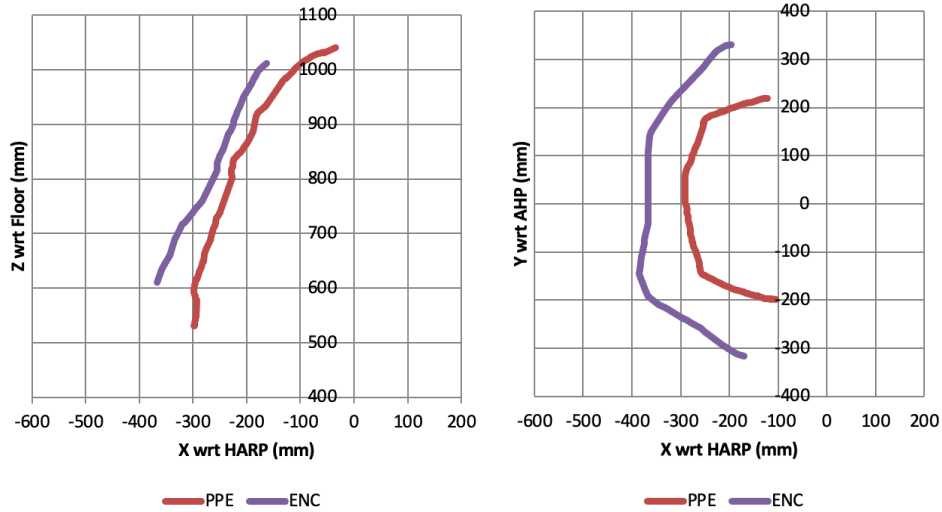


Figure 18. Torso contours relative to HARP in sideview (left) and top view (right).

### *Keyboard Position -- Preferred*

In each test condition, the participant selected their preferred vertical and fore-aft position for the keyboard. The distribution of the locations of the keyboard home row is modeled in this report. The calculations are very similar to those for seat position in driver positions (see Zerehsaz et al. 2014a). The location relative to the HARP and floor is influenced by anthropometry and ensemble level (see posture prediction equations, above). Fore-aft and vertical location are modeled independently because no correlation was noted between these variables. Figure 19 shows an example adjustment range to accommodate 90% of the ANSUR II population.

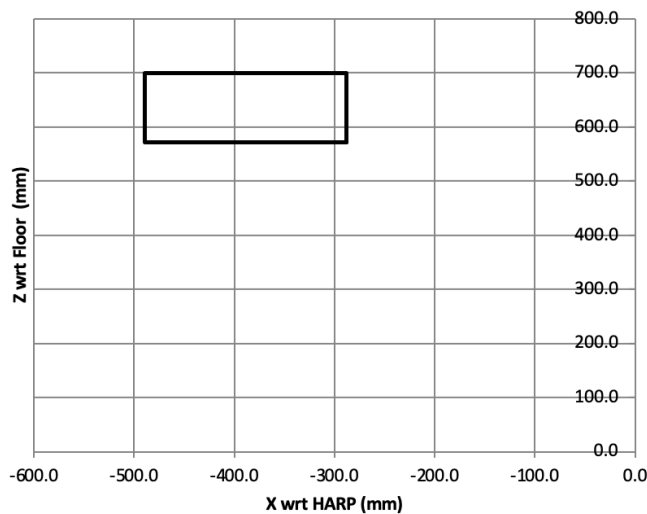


Figure 19. Keyboard home row adjustment range with respect to HARP to accommodate preferred positions.



### *Keyboard Position – Acceptable Range*

To model the acceptable range, the distribution of maximum forward and maximum rearward positions were modeled separately. The front and rear cutoffs were chosen such that the calculated range would result in the target percentage of the population being able to find a position within their acceptable range. That is, the *rear* of the travel was computed using the *forward* acceptable location distribution, and the *front* of the travel was computed using the *rearward* acceptable location distribution. Because the acceptable range was measured only for fore-aft position, the vertical range of preference was also assumed to be the range of acceptability. Comparing Figures 19 and 20, the acceptable range is much smaller than the preferred range of adjustment.

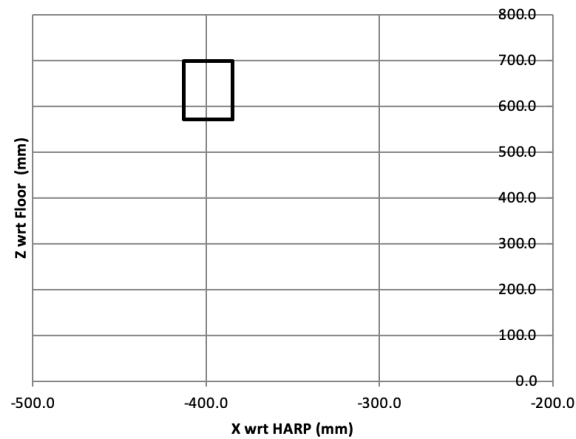


Figure 20. Acceptable keyboard home row range.

### *Screen Position – Preferred*

The preferred fore-aft screen position was modeled in the same manner as the keyboard preferred position. Because the vertical position was fixed, only the fore-aft location is modeled. Figure 21 shows preferred range for 90% accommodation relative to HARP and the floor. Note that the vertical extent of the screen depiction in Figure 21 is the height of the screen used in the data collection and does not constitute design guidance.

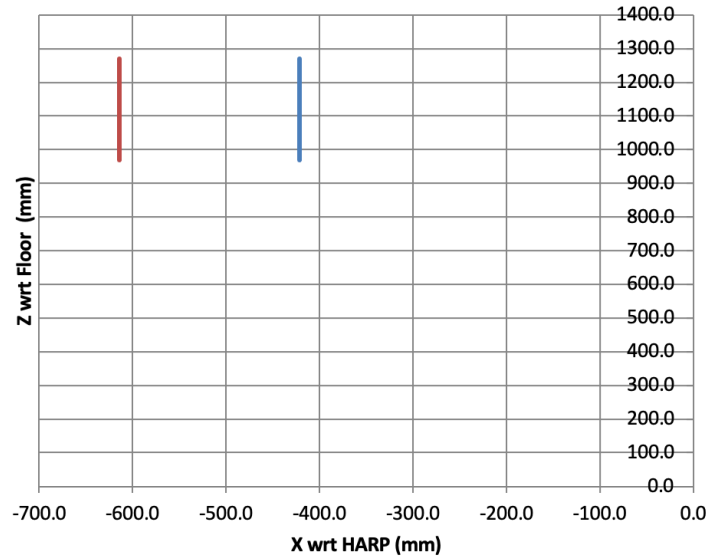


Figure 21. Preferred range of fore-aft screen position for 90% accommodation. Vertical extent shows the screen height used in the study is not a model output or recommendation.

### *Screen Position – Acceptable*

The acceptable range of fore-aft screen adjustment was modeled in the same manner as the keyboard acceptable position. Figure 22 shows acceptable range for 90% accommodation relative to HARP and the floor.

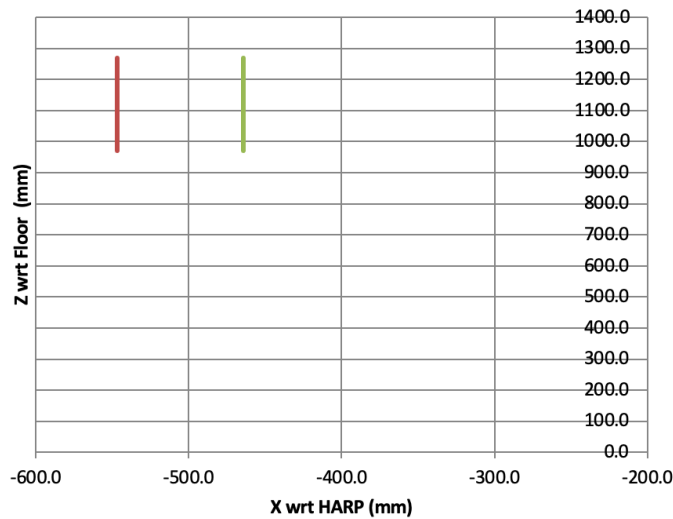


Figure 22. Acceptable range of fore-aft screen position for 90% accommodation. Vertical extent shows the screen height used in the study is not a model output or recommendation.

### Helmet Contour

In prior work, the average front- and side-view profiles of the advanced combat helmet (ACH) relative to the eye and head centerline were documented (see Appendix D). For the current work, the side and rear-view contours were positioned with respect to the centroid of the eyellipse, in the same manner as for other seating positions for which eyellipses were generated. The centroid of the contour is located 82.5 mm forward of and 75.8 mm above the eyellipse centroid. The front of the contour is 52.2 mm forward of the front of the eyellipse, the top is 161.8 mm above the top of the eyellipse, and the rear is 217.1 mm behind the rear of the eyellipse.

The lateral margin of the cutoff included the lateral half-width of the cyclopean contour of 129.9 mm positioned with respect to each eye location, taking into account the eyellipse width and assuming the standard 65-mm interpupillary breadth. A 23-mm head turn allowance derived from SAE J1052 was added to both sides of the contour.

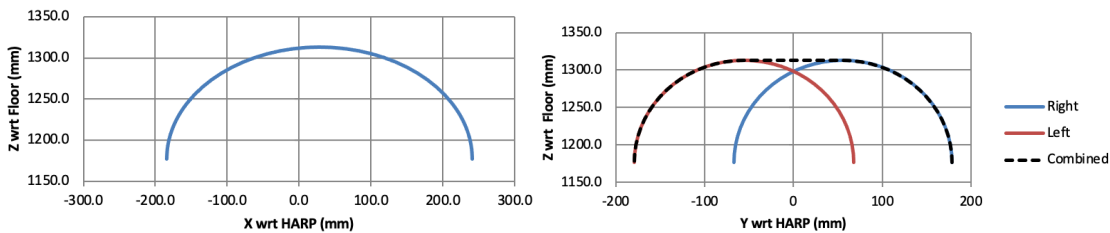


Figure 23. Helmet cutoff contours for 95% accommodation: side view (left) and rear view (right).

### Knee Contour

Knee clearance contours are based on modeling of the location of the suprapatellar landmark with respect to the eye (X), seat centerline (Y), and HARP (Z). The mean vertical location of the HARP is added to express the result relative to the floor.

Using the same methods applied for other landmarks, a 3D cutoff ellipse is computed for the suprapatellar landmark (Figure 24). The leg segment angle was set to vertical and the thigh segment angle with respect to horizontal was computed from the corresponding regression equation. A tibia landmark location is computed using the offset of  $\{-22, -47\}$  mm with respect to the suprapatellar landmark. The X and Z axes of the contour are extended downward and forward to accommodate the tibia landmark and a new centroid is computed. A standard knee width of 110 mm is used to extend the ellipse laterally. Finally, tangents to the ellipse at the tibia and thigh segment angles are constructed in side-view to represent the front of the leg and top of the thigh.

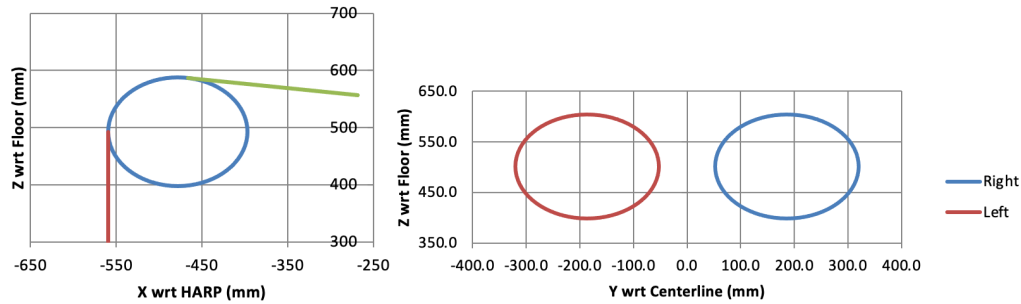


Figure 24. Sideview (left) and rearview (right) knee contours.

### Elbow Contour

Elbow clearance contours were created based on modeling the lateral humeral epicondyle landmark location, with adjustments for the olecranon process (Figure 25). Elbow location was modeled with respect to the HARP (X & Z) and seat centerline (Y). The elbow contour is affected by anthropometry and ensemble level. Using the same process as for other contours, the centroid is computed from the mean anthropometry values for men and women and adjusted for ensemble level (Y and Z only). The vertical axis length was extended downward by 35 mm to accommodate the olecranon process.

Resting elbow contours were also added that are based on the squad model (Zerehsaz et al. 2014b). The squad model takes seat back angle as an input. For the current modeling, the mean predicted seat back angles of men and women were used.

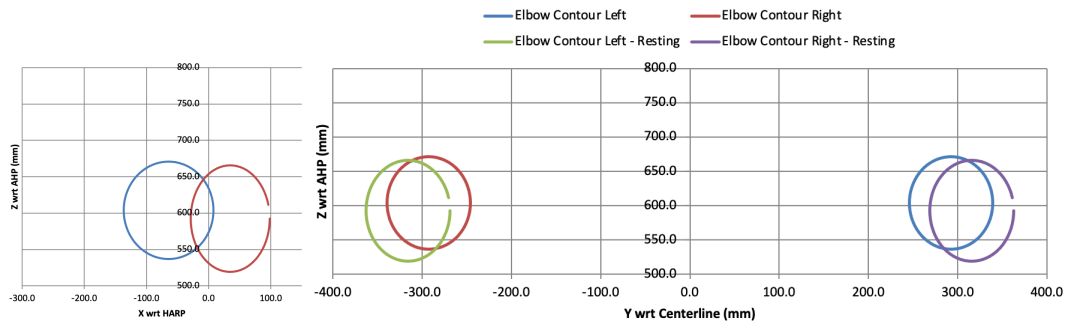


Figure 25. Commander elbow contours in sideview (left) and rear view (right). Contours are shown for both keyboard use and resting. The resting contours are more rearward and outward.

### Boot Contour

Boot contours were generated to account for clearance in front of the occupant. The legs were assumed to be vertical so that the ankles were directly under the knees. The toe centroid was estimated based on data from Reed and Ebert (2020) as  $51.9 + 0.0925 * \text{Stature}$ . The standard methods for estimating the forward boundary that accounted for 95% of toe points were used. A toe ellipsoid was generated in X and Y (i.e., on the floor) using the knee lateral axis length. The vertical axis was then set to extend 125 mm (approximately 5 inches) above the floor, and 100 mm (approximately 4

inches) was added to the lateral extent to provide accommodation for the boot. The contour was the extended rearward from the top of the toe box to the knee X coordinate. Figure 26 shows the resulting contours.

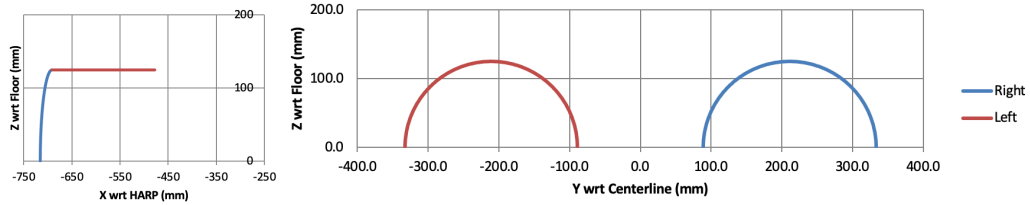


Figure 26. Commander boot contours in sideview (left) and rear view (right).

## Accommodation Models for Gunner Position

### Inputs

In addition to variables listed above for the commander models, the (fixed) seat back angle is an input to the gunner models. For this illustration, the seat back angle was set to 10 degrees, with no hydration pack relief. Calibration was J826.

### Outputs

Figure 27 illustrates the contours generated by the gunner accommodation models in sideview. Figure 28 shows the contours in top view to demonstrate the joystick adjustment ranges.

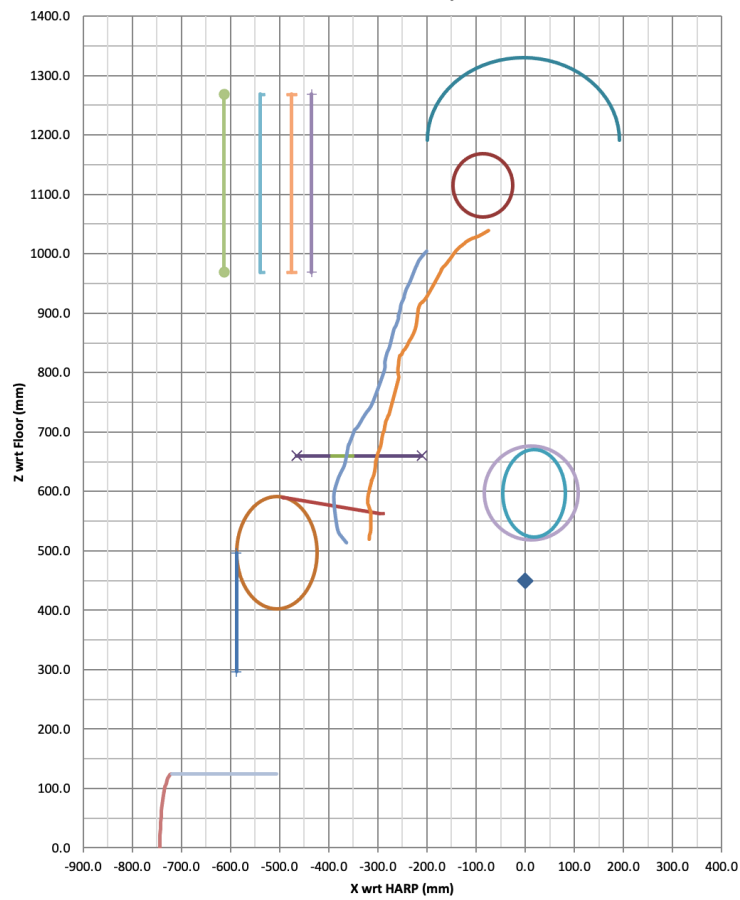


Figure 27. Outputs for the gunner accommodation models in sideview.

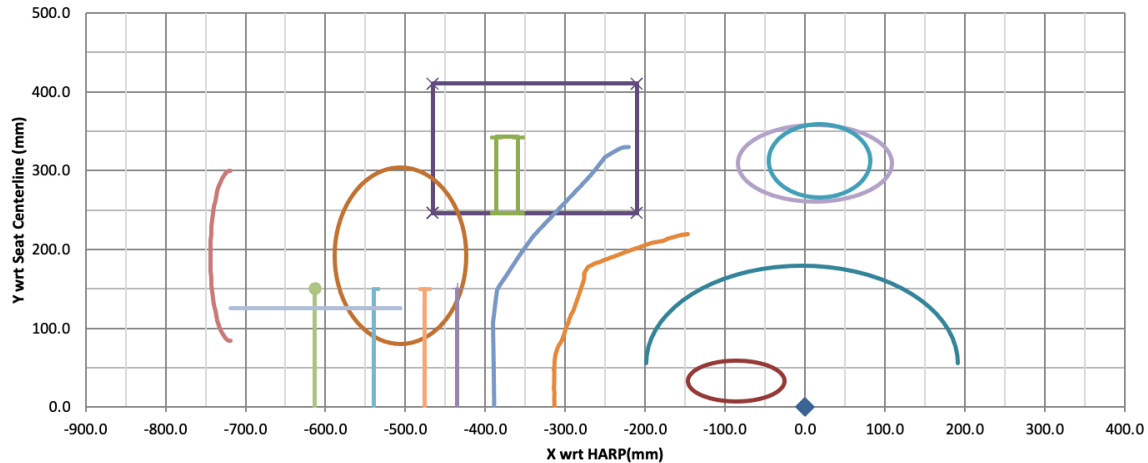


Figure 28. Outputs for the gunner accommodation models in top view. Only the right side is shown.

### *Eyellipse*

The eyellipse was constructed in the same manner as for the commander position using the equations for eye location with respect to HARP from Table 12. Note that seat back angle is an input for the gunner position, rather than an output as for the commander position.

### *Torso Contour*

Torso contours were constructed in the same manner as for the commander position, using the HARP location as the reference. The torso contours were rotated relative to the original driver model based on the mean hip-to-eye angle.

### *Joystick*

The preferred and acceptable joystick positions were modeled in a manner similar to the procedures used for the keyboard. The vertical joystick location was fixed, so the calculations are performed in the horizontal plane. A 95% accommodation boundary was computed for the preferred position. For the acceptable range, the inboard edge was determined using the preferred range, while the forward, rearward, and outboard edges were determined from the maximum acceptable data.

### *Helmet Contour*

Helmet contours were calculated identically to the contours for the commander position.

### *Knee Contour*

Knee contours were calculated using the same methods applied for the commander position.

*Elbow Contour*

Elbow contours were calculated using the same methods applied for the commander position. Resting elbow contours were calculated using the seat back angle as input.

*Boot Contour*

Boot contours were calculated using the same methods applied for the commander position.



## **DISCUSSION**

This report presents the first data-based posture prediction and accommodation models for commander and gunner positions in military vehicles. The prior squad models were also for non-driver positions (Zerehsaz et al. 2014b) but those models did not include data on the locations of the relevant controls and displays. The data are based on a large, diverse sample of Soldiers, and the models are parametric so that they can represent a wide range of current and future warfighter populations. The new models include the effects of two ensemble levels.

### **Limitations and Future Work**

These results are limited in several ways by the data collection environment and protocols. In addition to minimally contoured, artificial seats, the data were gathered during short-duration sitting sessions (a few minutes in each test condition), and the laboratory environment lacked many of the other spatial constraints of military vehicle. However, the goal of the current work was to establish the space requirements and adjustment preferences without those constraints for use in design. The conditions did not include realistic tasks; only the physical requirements of those tasks were simulated. No dynamic ride motion was present.

The two most important limitations of the models are the unknown dependence on the clothing/gear ensembles and seats. Different body armor designs, for example with thicker or thinner plates, could affect torso posture and position. Seat design could also influence posture and position and could interact with the body armor design. A study is underway to address these issues.

## REFERENCES

Gordon, C. C., Blackwell, C. L., Bradtmiller, B., Parham, J. L., Barrientos, P., Paquette, S. P., and Mucher, M. (2014). 2012 Anthropometric Survey of Marine Corps Personnel: Methods and Summary Statistics. (NATICK/TR-15/007). Army Natick Soldier Research Development and Engineering Center, Natick, MA.

Reed, M.P. and Ebert, S.M (2013). The Seated Soldier Study: Posture and Body Shape in Vehicle Seats. Technical Report UMTRI-2013-13. University of Michigan Transportation Research Institute, Ann Arbor, MI.

Reed, M.P. and Ebert, S.M (2020). Development of Driver Posture Prediction and Accommodation Models for Military Vehicles: Fixed-Eye-Point, Out-of-Hatch, and Highly Reclined Driver Configurations. Technical Report UMTRI-2020-5. University of Michigan Transportation Research Institute, Ann Arbor, MI.

Zerehsaz, Y., Ebert, S.M., and Reed, M.P. (2014a). Development of Accommodation Models for Soldiers in Vehicles: Driver. Technical Report UMTRI-2014-26. University of Michigan Transportation Research Institute, Ann Arbor, MI.

Zerehsaz, Y., Ebert, S.M., and Reed, M.P. (2014b). Development of Accommodation Models for Soldiers in Vehicles: Squad. Technical Report UMTRI-2014-39. University of Michigan Transportation Research Institute, Ann Arbor, MI.









- *If their legs or ankles are crossed ask them to uncross them. If they say that this is how they usually or prefer to sit say - I understand, but for this study we ask that everyone sit with their legs and ankles uncrossed.*
- *Further explanation if needed - We are not measuring your personal preference in this study, but rather how Soldiers of different shapes and sizes fit in seats.*

## APPENDIX B GENERAL CALCULATION METHODS FOR ACCOMMODATION MODELS

This section closely follows presented previously (Zerehsaz et al 2014a, 2014b).

### *Convolving Normal Distributions with Linear Models*

The data analysis and model development in this report are based on linear regression analysis and exploit some of the statistical characteristics of linear functions of variables that follow a normal distribution. In general, a dimension of interest, such as fore-aft seat position, is expressed as a linear function of potential predictors, such as seat height and driver stature. The models have the form

$$y = c_0 + c_1 x_1 + c_2 x_2 + \dots + e(0, s^2) \quad [B1]$$

where  $y$  is the dependent measure to be predicted, the  $c_i$  are constant coefficients obtained by fitting to the data, the  $x_i$  are the predictors (vehicle and driver body dimensions). The final “error” term  $e(0, s^2)$  is a random, normally distributed variable with zero mean and variance  $s^2$ , where  $s$  is the root mean square error (RMSE) of the regression. In computational terms, the RMSE is the standard deviation of the data vector that is obtained by subtracting the regression prediction from each data observation. This residual variance is a crucial part of the modeling in this report.

The model development procedure in this report exploits an important feature of normal distributions, which is that the mean and standard deviation of a linear function of a normal distribution is also a normal distribution. Specifically, if

$$Y = c_0 + c_1 X \quad [B2]$$

where  $c_0$  and  $c_1$  are constants and  $X$  is a normal distribution with mean  $X_{\text{Mean}}$  and standard deviation  $s_X$ , then  $Y$  is also a normal distribution, with mean

$$Y_{\text{Mean}} = c_0 + c_1 X_{\text{Mean}} \quad [B3]$$

and variance (standard deviation squared) of

$$s_Y^2 = (c_1 s_X)^2 \quad [B4]$$

The sum of two normal distributions is also a normal distribution, with variance equal to the sum of the variances. So, the residual variance from a regression can be included in estimating the distribution of the dependent measures. For example, consider

$$HARPX = c_0 + c_1 \text{Stature} + e(0, s^2) \quad [B5]$$

where  $HARPX$  is driver-selected fore-aft seat position,  $c_0$  and  $c_1$  are constant coefficients from the regression analysis, and  $s$  is the root mean square error from the regression. If stature is modeled as a normally distributed random variable, this becomes the sum of



two normally distributed random variables. Hence, for this example, *HARPX* is modeled as a normal distribution with mean

$$HARPX_{\text{Mean}} = c_0 + c_1 \text{Stature}_{\text{Mean}} \quad [\text{B6}]$$

and variance

$$s_{\text{Stature}}^2 = (c_1 s_{\text{Stature}})^2 \quad [\text{B7}]$$

This formulation is particularly valuable for modeling driver posture because the relevant human descriptors, such as stature and body mass index, are approximately normally distributed within gender or can be transformed to be. If the predictors are correlated, then the calculation of the variance of the independent is slightly different. For the equation

$$Y = c_1 X_1 + c_2 X_2 \quad [\text{B8}]$$

where  $X_1$  and  $X_2$  are normally distributed random variables with variances  $s_1^2$  and  $s_2^2$  and correlation  $r_{1,2}$ , the variance of  $Y$  is given by

$$s_Y^2 = (c_1 s_1)^2 + (c_2 s_2)^2 + 2 r_{1,2} s_1 s_2 \quad [\text{B9}]$$

For a difference between two normal random variables

$$Y = c_1 X_1 - c_2 X_2 \quad [\text{B10}]$$

the covariance ( $r_{1,2} s_1 s_2$ ) is subtracted:

$$s_Y^2 = (c_1 s_1)^2 + (c_2 s_2)^2 - 2 r_{1,2} s_1 s_2 \quad [\text{B11}]$$

In general, the occupant population includes both men and women. Although single-gender distributions of many anthropometric variables can be accurately approximated as normal distributions, the male and female components must usually be modeled separately. The level of accommodation for each gender is computed and the respective fractions are combined using the population gender mix. For example, if the fraction of males in the population is  $m$ , the total fraction accommodated is

$$F_{\text{total}} = m (F_m) + (1-m) F_f \quad [\text{B12}]$$

where  $F_m$  and  $F_f$  are the fractions of male and female occupants accommodated, respectively.

### *Cutoff Concept*

To construct geometric contours that represent accommodation models, we want to identify “cutoff points” beyond which a desired percentage of the population lies. For example, we may want to construct a contour such that 95% of heads lie below a tangent to the contour. To identify cutoff points on each axis of interest, we calculate the mean and standard deviation of the individual male and female populations, then iteratively

find the location (an X, Y, or Z coordinate value) such that the combined population is appropriately divided at the cutoff point. Note that for a single-sex population approximated by a normal distribution we can immediately calculate the cutoff in closed form from the cumulative normal distribution, but for the combined population we must iterate, applying the male/female distribution (for example, 90% male).

### *Computing Cutoffs in Excel*

The Excel spreadsheets accompanying this report use the function NORMDIST to model the combined male and female population distribution. The function representation of equation B12 is

```
=FractionMale*NORMDIST(cutoff_value, male_mean, male_standard_deviation, 1) + (1-FractionMale)*NORMDIST(cutoff_value, female_mean, female_standard_deviation, 1)
```

where the means and standard deviations are the values computed for the distribution of interest (for example, front of seat track travel). The last argument to the NORMDIST function is a 1 to indicate that the cumulative function is to be used. The cutoff value is iterated using the Goal Seek functionality in Excel to achieve the desired percentage cutoff (e.g., 5% for 95% accommodation).

## APPENDIX C

### DRIVER ANTERIOR TORSO CONTOURS

All coordinates in mm.

#### Rifleman (ENC/BBG) Side View Relative to Reference Point

X	Z
210.7	269.7
201.3	262.2
193.1	254.7
187.7	246.2
186.5	245.1
180.1	234.3
171.6	219.9
163.8	209.3
158.7	198.6
157.9	195.5
150.9	184.4
148.4	175.9
143.9	166.2
144.1	164.9
144.2	164.6
143.5	161.1
137.0	149.1
133.0	144.3
121.4	115.3
115.7	106.1
109.7	90.7
107.9	77.6
77.5	22.3
64.6	8.9
58.4	2.2
56.0	-0.4
50.9	-6.8
43.5	-14.8
38.1	-18.5
34.4	-25.3
25.4	-40.6
23.8	-42.2
13.5	-73.3
4.5	-87.0
-3.2	-99.1
-12.7	-121.2
-14.1	-143.1
-14.1	-143.1
-12.7	-165.8
-9.9	-185.8
-2.8	-196.3
5.3	-206.3

**Rifleman (ENC/BBG) Top View Relative to Reference Point (Z Value is -121 mm)**

X	Y
157.3	401.9
147.2	400.3
128.1	389.4
125.2	386.0
110.4	367.3
100.0	355.8
39.2	291.0
31.8	281.2
17.4	260.7
4.1	239.9
-7.5	222.1
-9.5	212.3
-13.6	178.5
-13.4	177.6
-12.3	30.0
-19.4	5.1
-20.5	-2.2
-20.1	-10.6
-26.1	-33.1
-26.7	-39.1
-30.0	-65.3
-31.4	-72.7
-31.4	-72.7
-18.6	-106.6
-13.1	-120.3
8.5	-138.4
23.3	-143.5
58.9	-165.9
65.9	-169.3
76.0	-174.7
95.9	-187.1
103.5	-194.7
107.6	-197.4
138.3	-220.7
169.1	-239.3
183.4	-244.6

**IOTV Side View Relative to Reference Point (PPE Ensemble Level)**

X	Z
-138.3	-344.8
-137.9	-344.3
-137.3	-338.9
-135.2	-334.4
-133.8	-329.3
-131.1	-298.7
-132.0	-296.4
-133.3	-292.7
-134.1	-289.6
-134.7	-288.1
-136.1	-284.5
-135.6	-280.4
-135.7	-280.0

-135.3	-276.6
-134.0	-271.7
-133.7	-269.7
-132.6	-267.3
-131.7	-266.1
-130.1	-260.0
-129.8	-259.8
-125.1	-248.0
-124.9	-246.4
-120.0	-239.2
-116.0	-228.0
-115.7	-227.0
-113.5	-214.8
-113.1	-214.8
-108.5	-203.5
-107.5	-201.1
-101.2	-190.1
-97.8	-178.3
-94.5	-168.8
-92.4	-165.7
-91.6	-163.6
-89.7	-157.0
-89.1	-155.8
-87.1	-149.6
-85.0	-146.9
-82.0	-141.3
-81.7	-140.8
-80.1	-139.9
-79.8	-139.2
-54.4	-78.7
-54.7	-75.6
-55.4	-70.1
-54.7	-62.9
-53.5	-58.8
-53.0	-57.7
-52.2	-51.1
-50.2	-44.4
-48.9	-42.1
-47.8	-41.5
-45.3	-40.6
-41.8	-35.1
-38.7	-33.1
-36.1	-30.4
-33.3	-27.4
-31.0	-24.1
-26.8	-18.3
-25.8	-17.9
-19.0	-8.9
-11.8	5.0
-4.7	33.4
-3.7	34.8
-3.0	35.6
-1.2	39.5
3.3	43.3
3.5	43.4
5.3	43.6
12.0	49.3
13.3	49.8

46.4	91.5
47.6	94.1
48.4	95.3
50.1	97.0
53.1	99.1
54.0	99.8
55.1	100.8
57.6	102.4
63.2	107.5
66.1	110.1
68.2	111.9
70.9	114.6
75.6	119.3
80.3	123.4
85.5	127.2
89.2	129.6
94.0	132.0
94.8	132.5
99.5	135.0
101.9	136.7
109.5	139.7
115.1	141.4
118.8	142.0
126.6	143.6
127.3	143.4
149.4	151.8

**IOTV Top View Relative to Reference Point (PPE Ensemble Level)**

X	Y	Z
58.7	-198.7	-250
48.9	-197.6	-250
48.3	-198.0	-250
45.2	-197.4	-250
36.3	-196.4	-250
34.0	-195.6	-250
28.2	-194.2	-250
27.6	-194.2	-250
22.2	-191.5	-250
16.3	-190.0	-250
15.8	-190.2	-250
12.1	-189.0	-250
10.1	-188.7	-250
1.7	-186.4	-250
-0.6	-185.9	-250
-1.5	-185.3	-250
-4.8	-183.8	-250
-6.1	-183.5	-250
-14.2	-181.8	-250
-18.7	-180.4	-250
-25.5	-178.0	-250
-32.1	-174.8	-250
-34.9	-174.2	-250
-40.3	-171.4	-250
-48.4	-168.0	-250
-51.7	-167.0	-250
-52.8	-166.4	-250

-57.9	-163.8	-250
-63.6	-161.2	-250
-66.9	-159.9	-250
-71.8	-156.7	-250
-75.8	-154.2	-250
-79.5	-153.0	-250
-86.6	-149.2	-250
-88.5	-148.2	-250
-90.7	-147.0	-250
-91.7	-146.1	-250
-92.5	-144.8	-250
-94.1	-141.9	-250
-95.2	-139.0	-250
-95.4	-137.7	-250
-95.7	-134.9	-250
-96.9	-131.4	-250
-96.9	-130.2	-250
-97.3	-123.4	-250
-105.7	-97.8	-250
-109.2	-89.1	-250
-111.7	-79.3	-250
-112.3	-77.2	-250
-113.0	-73.0	-250
-115.4	-63.9	-250
-115.4	-57.5	-250
-116.8	-52.1	-250
-118.2	-46.2	-250
-119.1	-37.8	-250
-120.1	-34.6	-250
-121.3	-25.8	-250
-121.7	-23.2	-250
-123.3	-16.8	-250
-122.9	-11.9	-250
-124.0	-6.5	-250
-124.4	-5.1	-250
-126.6	2.0	-250
-126.6	8.2	-250
-126.9	10.7	-250
-126.4	17.5	-250
-127.3	24.8	-250
-127.0	26.8	-250
-127.0	28.3	-250
-126.7	44.4	-250
-127.2	46.5	-250
-126.8	47.7	-250
-126.3	58.9	-250
-125.1	67.0	-250
-125.1	67.0	-250
-121.9	76.8	-250
-119.7	80.3	-250
-116.7	85.4	-250
-116.6	86.1	-250
-115.2	90.1	-250
-115.1	90.4	-250
-115.1	90.8	-250
-113.5	94.4	-250
-112.3	99.9	-250
-108.7	107.9	-250

-108.4	110.5	-250
-107.0	113.1	-250
-105.4	117.7	-250
-102.6	122.4	-250
-89.4	160.9	-250
-89.0	163.7	-250
-88.8	166.4	-250
-89.3	168.3	-250
-88.2	171.0	-250
-84.7	176.9	-250
-82.8	178.5	-250
-78.9	180.3	-250
-75.8	182.2	-250
-75.3	182.6	-250
-70.4	183.7	-250
-64.2	186.4	-250
-57.8	188.6	-250
-54.9	189.9	-250
-53.8	190.2	-250
-51.1	191.1	-250
-50.2	191.4	-250
-39.6	195.5	-250
-33.7	197.8	-250
-25.3	200.8	-250
-23.6	201.0	-250
-19.1	202.8	-250
-6.5	207.3	-250
0.4	209.0	-250
11.1	211.0	-250
15.5	213.2	-250
24.1	215.7	-250
34.9	218.7	-250
35.2	218.7	-250
38.6	218.8	-250
41.8	219.4	-250



## APPENDIX D

### HELMET CONTOURS

Relative to Eye and Head Centerline

Sagittal		Coronal		
X	Z	Y	Z	
-52.2	53.4	-129.9		-11.0
-51.8	56.7	-129.0		-5.3
-51.2	60.0	-128.1		0.2
-50.6	63.3	-127.2		5.7
-50.0	66.4	-126.3		10.9
-49.3	69.5	-125.4		16.1
-48.6	72.5	-124.5		21.1
-47.8	75.5	-123.5		25.9
-47.0	78.4	-122.6		30.6
-46.1	81.2	-121.7		35.2
-45.2	83.9	-120.7		39.7
-44.3	86.6	-119.8		44.0
-43.3	89.2	-118.8		48.2
-42.3	91.8	-117.9		52.3
-41.3	94.3	-116.9		56.3
-40.2	96.7	-115.9		60.1
-39.0	99.1	-114.9		63.8
-37.9	101.4	-113.9		67.5
-36.7	103.7	-112.9		71.0
-35.4	105.9	-111.9		74.4
-34.2	108.1	-110.9		77.7
-32.9	110.2	-109.9		80.9
-31.5	112.2	-108.9		84.0
-30.2	114.2	-107.8		87.0
-28.8	116.2	-106.8		89.9
-27.3	118.0	-105.8		92.8
-25.9	119.9	-104.7		95.5
-24.4	121.7	-103.6		98.1
-22.9	123.4	-102.6		100.7
-21.3	125.1	-101.5		103.2
-19.8	126.7	-100.4		105.6
-18.2	128.3	-99.3		107.9
-16.6	129.9	-98.2		110.1
-14.9	131.4	-97.1		112.3
-13.3	132.8	-96.0		114.4
-11.6	134.2	-94.8		116.4
-9.9	135.6	-93.7		118.3
-8.2	136.9	-92.6		120.2

-6.4	138.2	-91.4	122.0
-4.6	139.5	-90.3	123.7
-2.9	140.7	-89.1	125.4
-1.0	141.8	-87.9	127.1
0.8	143.0	-86.8	128.6
2.6	144.0	-85.6	130.1
4.5	145.1	-84.4	131.6
6.4	146.1	-83.2	133.0
8.2	147.1	-82.0	134.3
10.2	148.0	-80.7	135.6
12.1	148.9	-79.5	136.9
14.0	149.8	-78.3	138.0
16.0	150.6	-77.0	139.2
17.9	151.4	-75.8	140.3
19.9	152.2	-74.5	141.4
21.9	152.9	-73.3	142.4
23.9	153.6	-72.0	143.4
25.9	154.3	-70.7	144.3
27.9	154.9	-69.4	145.2
29.9	155.5	-68.1	146.1
31.9	156.1	-66.8	146.9
34.0	156.6	-65.5	147.7
36.0	157.1	-64.2	148.5
38.1	157.6	-62.9	149.2
40.1	158.1	-61.5	149.9
42.2	158.5	-60.2	150.6
44.2	158.9	-58.9	151.2
46.3	159.3	-57.5	151.8
48.4	159.6	-56.2	152.4
50.5	159.9	-54.8	152.9
52.5	160.2	-53.4	153.5
54.6	160.5	-52.0	154.0
56.7	160.7	-50.6	154.5
58.8	160.9	-49.3	155.0
60.9	161.1	-47.9	155.4
63.0	161.3	-46.4	155.8
65.1	161.4	-45.0	156.2
67.1	161.6	-43.6	156.6
69.2	161.6	-42.2	157.0
71.3	161.7	-40.8	157.3
73.4	161.8	-39.3	157.7
75.5	161.8	-37.9	158.0
77.6	161.8	-36.4	158.3
79.6	161.8	-35.0	158.6
81.7	161.7	-33.5	158.8
83.8	161.7	-32.0	159.1

85.8	161.6	-30.6	159.3
87.9	161.5	-29.1	159.6
89.9	161.4	-27.6	159.8
92.0	161.2	-26.1	160.0
94.0	161.1	-24.6	160.2
96.0	160.9	-23.1	160.4
98.1	160.7	-21.6	160.5
100.1	160.4	-20.1	160.7
102.1	160.2	-18.6	160.8
104.1	159.9	-17.1	161.0
106.1	159.6	-15.6	161.1
108.0	159.3	-14.1	161.2
110.0	159.0	-12.5	161.3
112.0	158.7	-11.0	161.4
113.9	158.3	-9.5	161.5
115.9	157.9	-7.9	161.6
117.8	157.5	-6.4	161.7
119.7	157.1	-4.8	161.7
121.6	156.6	-3.3	161.8
123.5	156.2	-1.7	161.8
125.4	155.7	-0.2	161.8
127.3	155.2	1.4	161.8
129.1	154.7	3.0	161.8
131.0	154.2	4.5	161.8
132.8	153.6	6.1	161.8
134.6	153.0	7.6	161.8
136.4	152.4	9.2	161.7
138.2	151.8	10.8	161.7
139.9	151.2	12.4	161.6
141.7	150.5	13.9	161.5
143.4	149.9	15.5	161.4
145.2	149.2	17.1	161.3
146.9	148.5	18.7	161.2
148.6	147.7	20.2	161.0
150.2	147.0	21.8	160.9
151.9	146.2	23.4	160.7
153.5	145.4	25.0	160.5
155.2	144.6	26.6	160.3
156.8	143.8	28.1	160.1
158.4	143.0	29.7	159.8
159.9	142.1	31.3	159.6
161.5	141.2	32.9	159.3
163.0	140.3	34.4	159.0
164.5	139.3	36.0	158.7
166.0	138.4	37.6	158.3
167.5	137.4	39.2	157.9

169.0	136.4	40.7	157.5
170.4	135.4	42.3	157.1
171.8	134.4	43.9	156.7
173.2	133.3	45.4	156.2
174.6	132.2	47.0	155.7
175.9	131.1	48.5	155.2
177.3	130.0	50.1	154.6
178.6	128.8	51.6	154.0
179.9	127.6	53.2	153.4
181.2	126.4	54.7	152.7
182.4	125.2	56.2	152.0
183.7	123.9	57.8	151.3
184.9	122.6	59.3	150.5
186.1	121.3	60.8	149.7
187.2	120.0	62.3	148.8
188.4	118.6	63.8	147.9
189.5	117.3	65.4	147.0
190.6	115.8	66.9	146.0
191.7	114.4	68.3	145.0
192.8	112.9	69.8	143.9
193.8	111.4	71.3	142.8
194.8	109.9	72.8	141.6
195.8	108.3	74.2	140.4
196.8	106.7	75.7	139.1
197.7	105.1	77.1	137.8
198.6	103.5	78.6	136.4
199.5	101.8	80.0	134.9
200.4	100.1	81.4	133.4
201.3	98.3	82.9	131.8
202.1	96.6	84.3	130.2
202.9	94.7	85.7	128.5
203.7	92.9	87.0	126.7
204.5	91.0	88.4	124.9
205.2	89.1	89.8	123.0
206.0	87.1	91.1	121.0
206.7	85.2	92.5	118.9
207.3	83.1	93.8	116.8
208.0	81.1	95.1	114.6
208.6	79.0	96.4	112.3
209.2	76.8	97.7	109.9
209.8	74.6	99.0	107.5
210.4	72.4	100.3	104.9
210.9	70.2	101.5	102.3
211.4	67.9	102.8	99.5
211.9	65.5	104.0	96.7
212.4	63.1	105.2	93.8

212.8	60.7	106.4	90.7
213.2	58.2	107.6	87.6
213.6	55.7	108.8	84.4
214.0	53.1	109.9	81.1
214.4	50.5	111.0	77.6
214.7	47.9	112.2	74.1
215.0	45.2	113.3	70.4
215.3	42.4	114.3	66.6
215.6	39.6	115.4	62.7
215.8	36.8	116.5	58.7
216.0	33.8	117.5	54.6
216.2	30.9	118.5	50.3
216.4	27.9	119.5	45.9
216.6	24.8	120.5	41.4
216.7	21.7	121.4	36.7
216.8	18.5	122.4	31.9
216.9	15.3	123.3	27.0
217.0	12.0	124.2	21.9
217.0	8.7	125.1	16.7
217.0	5.3	125.9	11.3
217.1	1.8	126.7	5.8
217.0	-1.7	127.6	0.1
217.0	-5.3	128.3	-5.7
216.9	-8.9	129.1	-11.7